Title
Overtaking collision effects in a cw double-pass proton linac

Journal
Physical Review Accelerators and Beams, 20(12)

ISSN
1098-4402

Authors
Tao, Yue
Qiang, Ji
Hwang, Kilean

Publication Date
2017-12-01

DOI
10.1103/physrevaccelbeams.20.124202

Peer reviewed

Overtaking collision effects in a cw double-pass proton linac

Yue Tao,[1,2,3] Ji Qiang,[2,*] and Kilean Hwang[2]

[1]*Institute of Modern Physics, Chinese Academy of Sciences, Lanzhou 73000, China*
[2]*Lawrence Berkeley National Laboratory, Berkeley, California 94720, USA*
[3]*University of Chinese Academy of Sciences, Beijing 100049, China*

(Received 4 August 2017; published 22 December 2017)

The recirculating superconducting proton linac has the advantage of reducing the number of cavities in the accelerator and the corresponding construction and operational costs. Beam dynamics simulations were done recently in a double-pass recirculating proton linac using a single proton beam bunch. For continuous wave (cw) operation, the high-energy proton bunch during the second pass through the linac will overtake and collide with the low-energy bunch during the first pass at a number of locations of the linac. These collisions might cause proton bunch emittance growth and beam quality degradation. In this paper, we study the collisional effects due to Coulomb space-charge forces between the high-energy bunch and the low-energy bunch. Our results suggest that these effects on the proton beam quality would be small and might not cause significant emittance growth or beam blowup through the linac. A 10 mA, 500 MeV cw double-pass proton linac is feasible without using extra hardware for phase synchronization.

DOI: 10.1103/PhysRevAccelBeams.20.124202

I. INTRODUCTION

The high-power proton linac has many applications in science and industry. For example, it is being studied as a driver for a subcritical nuclear power plant [1–3]. It is also proposed as a driver for a spallation neutron source in basic energy science and for high flux neutrino production in a high-energy physics study [4,5]. However, these single-pass superconducting proton linacs are expensive. In order to reduce the cost of the superconducting proton linac, the number and the type of superconducting cavities are minimized in the design.

The recirculating superconducting electron linac has been under operation for many years, which proves that a recirculating linac is an effective way to reduce the number of cavities and to save operational cost [6,7]. The concept of a recirculating proton linac was recently proposed in Ref. [8] and is shown in Fig. 1. It accelerates the proton beam from 150 MeV to multiple GeVs using three sections of superconducting linacs. Each section of the linac uses a single type of 650 MHz five-cell elliptical superconducting cavity to accelerate the proton beam multiple times. The key difference between the recirculating proton linac and the electron linac is the existence of phase slippage in the proton linac. A synchronous condition proposed in Ref. [8] has to be satisfied in order to accelerate the proton beam multiple times using the same fixed rf phase inside a cavity.

In the first section of the proposed linac, the proton beam is accelerated from 150 to 500 MeV by passing through the linac two times. The start-to-end beam dynamics design and single bunch simulation of this section had been carried out in Ref. [9] with 40 mA current at 650 MHz rf frequency (the same amount of charge as 10 mA current at 162.5 MHz rf frequency). A schematic plot of the double-pass superconducting proton linac is shown in Fig. 2. It consists of a section of superconducting linac with 17 cavities, two arcs, and a straight beam transport line that has four bunching cavities to keep the beam longitudinally bunched.

The proton beam passes through the superconducting linac twice in the double-pass superconducting linac. By appropriately adjusting the separation distance between two accelerating cavities, the proton beam can be accelerated through the linac with a fixed rf design phase in both passes. For cw operation, the proton bunch with higher energy during the second pass of the linac will overtake and collide with the proton bunch with lower energy during the first pass of the linac at several locations. At these collision locations, in addition to the space-charge forces from the bunch itself, each bunch will also be subject to the

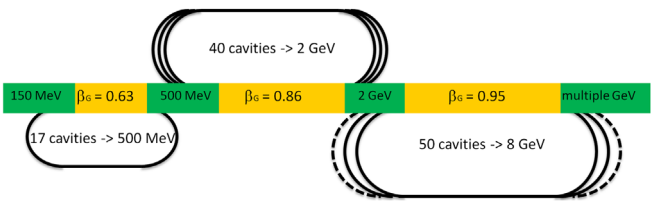

FIG. 1. A schematic plot of a GeV recirculating proton linac [8].

*jqiang@lbl.gov

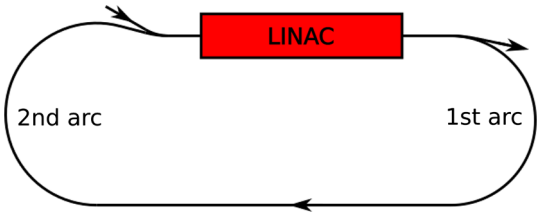

FIG. 2. Layout of the double-pass recirculating proton linac [9].

Coulomb space-charge forces from the other bunch. These space-charge forces from the other bunch may have detrimental effects on the beam quality and could cause beam emittance growth or blowup. The purpose of this paper is to investigate these collisional effects from space-charge forces through the double-pass linac using self-consistent beam dynamics simulations.

The organization of the paper is as follows: After the introduction, an analytic estimate of the catch-up collisional effects is discussed in Sec. II. The simulation results through a single catch-up collision region and through the entire linac are presented in Sec. III. The conclusion from this study is drawn in Sec. IV.

II. ANALYTICAL ESTIMATE OF THE EFFECTS OF OVERTAKING COLLISION

The Coulomb space-charge force in a high-intensity recirculating proton linac plays an important role in particle dynamics. The repulsive nonlinear space-charge force among protons reduces external focusing and can cause significant modification to the beam quality through the accelerator. To measure the strength of the space-charge effects in the proposed double-pass proton linac, we calculated the average tune depression from the phase advance without and with the space-charge effects. For the 40 mA beam (at 650 MHz) in this study, the tune depression is about 0.7. This suggests that the space-charge effects should have a significant impact on the proton beam dynamics in the proposed accelerator.

When the higher-energy proton bunch during the second pass of the linac catches up the lower-energy proton bunch during the first pass, there will be Coulomb interactions between these two bunches in addition to the space-charge forces within each bunch itself. The interaction Coulomb forces between two bunches are similar to the space-charge forces within the bunch itself and consist of the defocusing electric forces and the focusing magnetic forces. The focusing magnetic forces, which depend on the velocities, tend to compensate the defocusing forces from the electric fields. For example, for a proton inside the low-energy bunch, the radial Lorentz interaction force from the high-energy bunch during the collision can be given by

$$F_r^{H\to L} = q(E_r^H - \beta_L c B_\theta^H), \tag{1}$$

where q is the charge of the particle, E_r^H and B_θ^H are the electric and magnetic fields, respectively, from the high-energy proton bunch, c is the speed of light in a vacuum, and β_L is the velocity of the low-energy bunch (assuming a small velocity spread). Under the quasistatic approximation, the magnetic field can be written as

$$B_\theta^H(r) = \frac{\beta_H}{c} E_r^H(r), \tag{2}$$

where β_H is the high-energy bunch velocity. Combining Eqs. (1) and (2), the radial interaction space-charge forces between the high-energy bunch and the low-energy bunch during the overtaking collision can be written as

$$F_r^{H\leftarrow L,H\to L} = qE_r^{L,H}(1 - \beta_L\beta_H). \tag{3}$$

Here, $H \to L$ and $H \leftarrow L$ denote the space-charge force from the high-energy bunch to the low-energy bunch and from the low-energy bunch to the high-energy bunch, respectively, and $E_r^{L,H}$ the electric field of the low-energy bunch and the high-energy bunch respectively. Besides the space-charge forces from the overtaking collision, a proton is also subject to the space-charge forces within the bunch itself. The radial component of these space-charge forces can be written as

$$F_r^{L,H} = qE_r^{L,H}(1 - \beta_{L,H}^2). \tag{4}$$

For a three-dimensional uniform ellipsoidal beam, the electric fields are given as [10]

$$E_x = \frac{3I\lambda(1-f)}{4\pi\epsilon_0 c(r_x + r_y)r_z}\frac{x}{r_x}, \tag{5}$$

$$E_y = \frac{3I\lambda(1-f)}{4\pi\epsilon_0 c(r_x + r_y)r_z}\frac{y}{r_y}, \tag{6}$$

where the r_x, r_y, and r_z are the semiaxes of the ellipsoid which are related to the root mean square (rms) beam sizes a_i by $r_i = \sqrt{5}a_i$ $(i = x, y, z)$, I is the average current over an rf period, λ is the rf wave length, and f is the ellipsoid form factor and can be approximated as $f = 1/3p$ if $0.8 < p < 5$, where the form of parameter p is $p = \gamma r_z/\sqrt{r_x r_y}$.

The radial momentum change resulting from the space-charge forces can be approximated as

$$\Delta P_r = F_r \delta t, \tag{7}$$

where δt is the interaction time. The impact to the momentum change from the space-charge effects of the overtaking collision and from the space-charge effects within the bunch itself depends on both the Lorentz forces and the interaction time.

The space-charge Lorentz forces depend on the beam size and the particle velocity. For example, during the

TABLE I. Average rms beam sizes during interaction and through the accelerating cavity.

Time	Direction	Low bunch (mm)	High bunch (mm)
Interaction	X	2.25	1.81
	Y	1.50	1.31
	Z	1.20	1.81
Through	X	2.26	1.82
	Y	1.48	1.31
	Z	1.48	1.81

second collision (inside the fourth cavity), the average rms beam sizes during the interaction and through the accelerating cavity are given in Table I. It is seen that, in the same direction, the average beam size during the collision is similar to that through the accelerating cavity. The velocity difference between the lower-energy bunch and the higher-energy bunch is small, too. This suggests that the space-charge forces of those with a collision and those without a collision should be similar. The relative collisional effect on the momentum change also depends on the interaction time. Numerical simulation results show that the interaction time during the overtaking collision is 5.8×10^{-10} s, while inside the fourth cavity, the total time is about 4.9×10^{-9} s. Here, the interaction time is estimated from the longitudinal overlapping of two collisional bunches. Using the analytical space-charge field Eqs. (5) and (6), the rms beam sizes in Table I, and the interaction time, we estimate that the ratios of the low-energy bunch momentum change due to a single catch-up collisional effect to that due to the internal space-charge effects in the transverse direction (x and y) are about 14.5% and 13.1%, respectively. Following the same procedure, we estimate that the relative momentum change ratios for the high-energy bunch are about 10.3% and 11.1%. This suggests that the space-charge interaction effects during the overtaking collision might be somewhat small in comparison to the space-charge effects within the bunch itself and might not cause a dramatic change of beam quality after the collision.

III. NUMERICAL SIMULATION OF THE OVERTAKING COLLISIONAL EFFECTS

The collisional effects from the interbunch space-charge forces during the overtaking collision through the cw double-pass proton linac were investigated using self-consistent numerical beam dynamics simulations. Such detailed numerical simulations are necessary to evaluate the collisional effects during multiple collisions with dynamically evolving proton beam distributions.

A beam from a 162.5 MHz cw injector is directed to the double-pass recirculating proton linac, which consists of 17650 MHz five-cell superconducting elliptical cavities. There could be a maximum of five overtaking collision

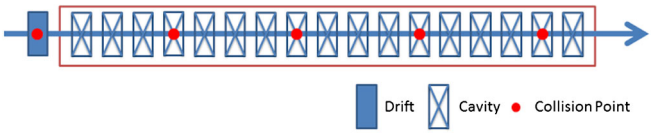

FIG. 3. A schematic plot of layout of the collision points in the linac.

locations during the cw operation. A layout of those collision points is shown in Fig. 3. The first collision occurs in a drift region in front of the linac. The remaining four collisions are inside four rf cavities, i.e., the fourth, the eighth, the twelfth, and the sixteenth cavity.

For a high-energy proton bunch during the second pass of the linac, it can catch up and collide with five different low-energy bunches still in the first pass. For a low-energy bunch during the first pass of the linac, it may collide with five different high-energy bunches. In this study, we assume that at the same collision location the differences among five high-energy or low-energy bunches are small and negligible. Thus, we will use a single low-energy bunch and a single high-energy bunch to collide five times in order to study the interbunch space-charge effects on the final beam quality. After the five collisions, the low-energy bunch proton beam is transported through the recirculating arcs and straight beam line and comes back to the superconducting linac section as a high-energy bunch for another five collisions during the second pass of the linac. There are a total of ten collisions for a proton bunch through the double-pass linac. The high-energy bunch proton beam used for the first five collisions is a beam that already experiences five collisions during the first pass of the linac.

We used the three-dimensional parallel beam dynamics code IMPACT-T [11] to simulate the space-charge effects during the two-bunch collision and the IMPACT-Z [12] code to simulate the individual beam bunch transport through the linac after the collision. The IMPACT-T code uses the time t as an independent variable in the simulation, while the IMPACT-Z code uses the longitudinal position z as an independent variable. Both codes employ a particle-in-cell (PIC) method to include the three-dimensional

TABLE II. Some physical parameters of low-energy and high-energy bunches at the entrance of collision regions.

Collision order	Bunch	Energy (MeV)	Phase (rad)
1	Low	150.00	338.76
	High	306.37	34.17
2	Low	165.85	85.90
	High	340.87	116.88
3	Low	195.88	203.66
	High	386.93	209.22
4	Low	236.26	337.90
	High	433.54	318.01
5	Low	282.24	138.22
	High	479.60	92.82

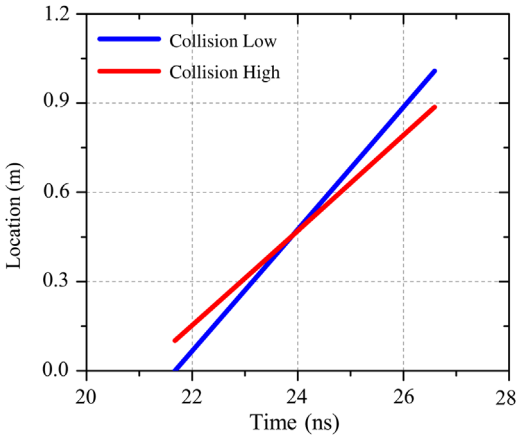

FIG. 4. Longitudinal bunch centroid evolution during an overtaking collision.

space-charge effects self-consistently. At the collision location, for each bunch, the space-charge fields from the bunch itself and the fields from the other bunch are summed together in the laboratory frame before interpolating to an individual particle. Here the space-charge fields of each bunch are obtained by solving the Poisson equation in each bunch beam frame and then transformed back to the laboratory frame following the Lorentz transformation. In the simulation, we have used 100 000 macroparticles for each bunch and $64 \times 64 \times 64$ numerical grid points. We checked the numerical convergence by doubling the number of macroparticles and grid points. Using the IMPACT-Z code to transport the beam outside the collisional region helps to reduce the computational time for the simulation through the entire system. Here, for each collision, the interaction region used in the simulation is the entire cavity or the drift space (for the first collision). In this region, the time-dependent PIC code IMPACT-T was used to simulate two-bunch evolution through the cavity including both the interbunch space-charge forces and the intrabunch space-charge forces. There is no transverse coherent effect in the simulation, since both bunches are on axis (no misalignment errors). The small longitudinal coherent effect was automatically included in the simulation from the interbunch space-charge forces. The time step size used during the collisional simulation is 1 ps, which is much smaller (10^{-3}) than the rf time period of the 650 MHz cavity. The initial distribution of the proton bunch is assumed to be a six-dimensional Gaussian distribution with rms emittances similar to those from the Project X design [4].

A. Collisional effects through a single interaction region

We first checked the space-charge effects on the proton beam quality after a single overtaking collision region. Some physical parameters of two Gaussian bunches before each collision are given in Table II. In order to study the interbunch space-charge effects during the collision, we first carried out a single-bunch beam dynamics simulation

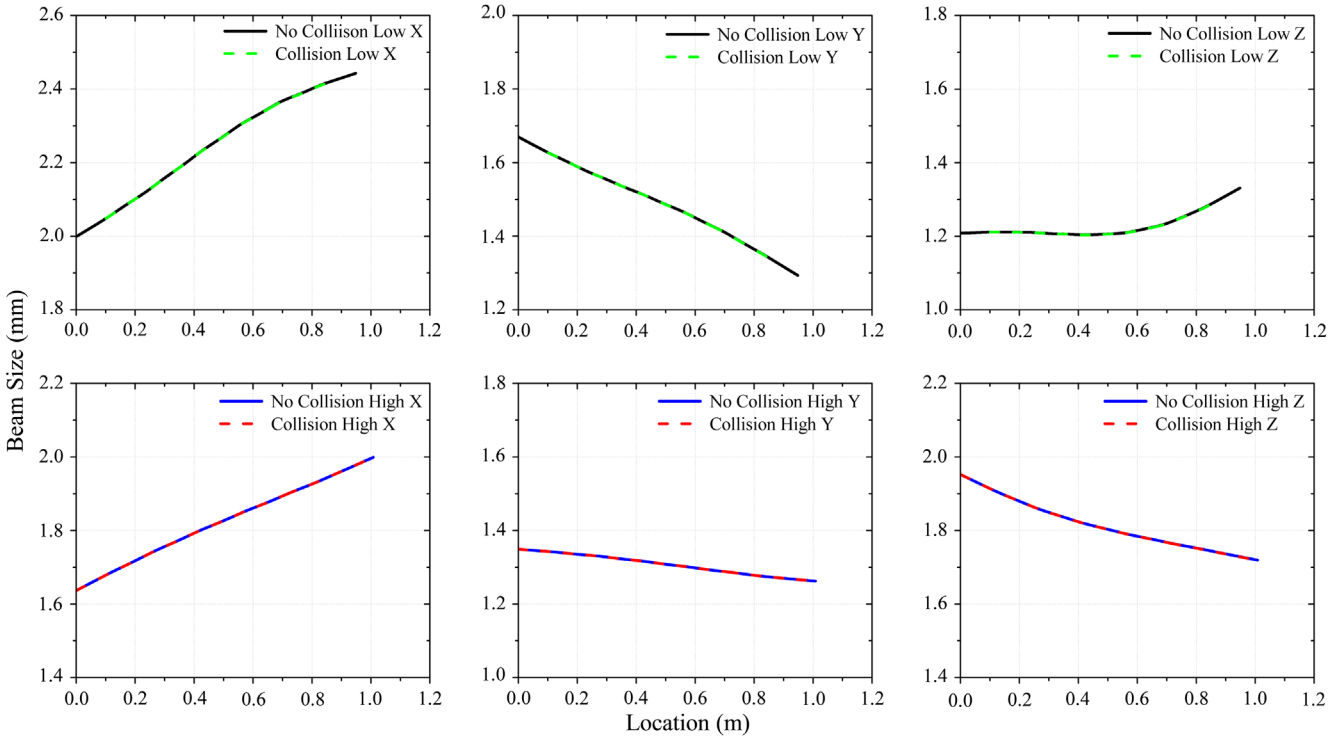

FIG. 5. The rms size evolution of the single-bunch simulation and the combined two -bunch simulation in the first cavity collision region.

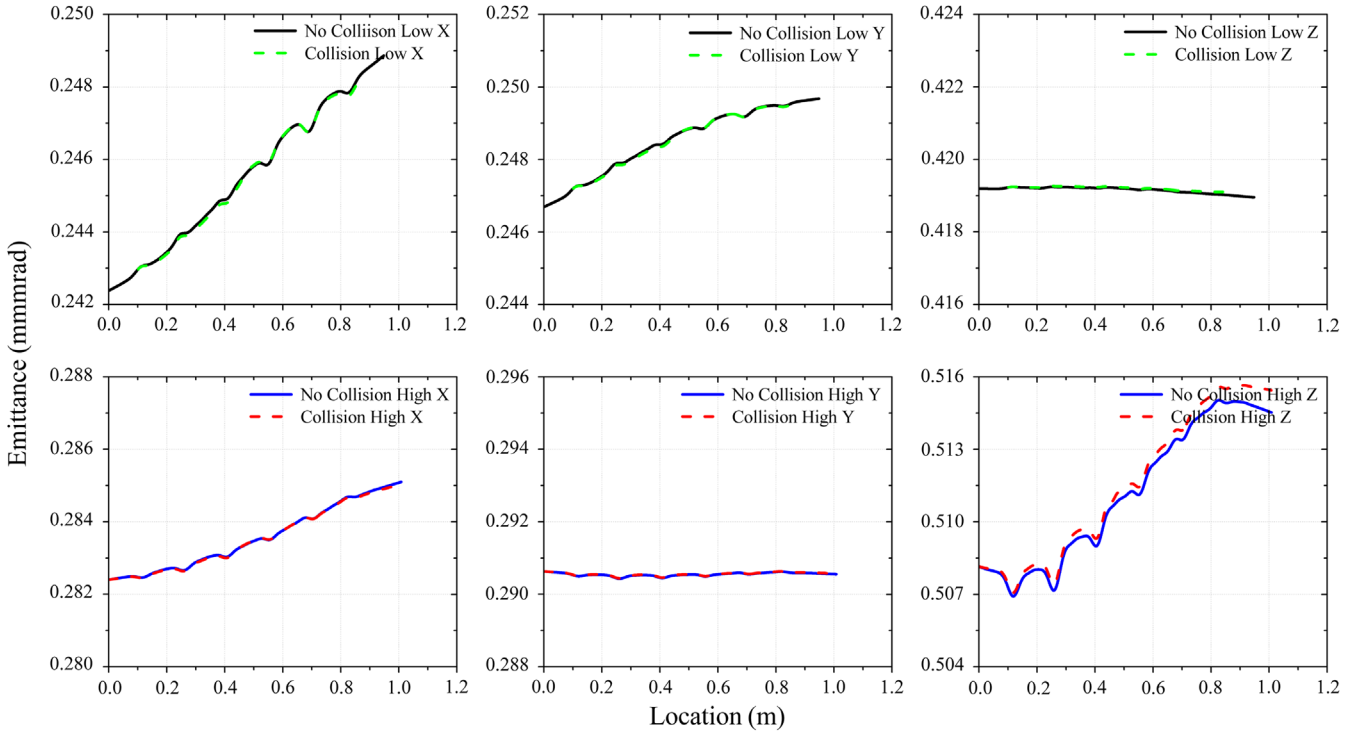

FIG. 6. The rms emittance evolution from the single-bunch simulation and the combined two -bunch simulation in the first cavity collision region.

through the linac using the IMPACT-Z code. Two particle distribution data files (one for the low-energy bunch and the other for the high-energy bunch) from the single-bunch simulation at a longitudinal location before the collision were used as the initial distributions. The overtaking collision process was simulated using the time-dependent self-consistent beam dynamics simulation IMPACT-T code. We converted the particle distribution from the IMPACT-Z

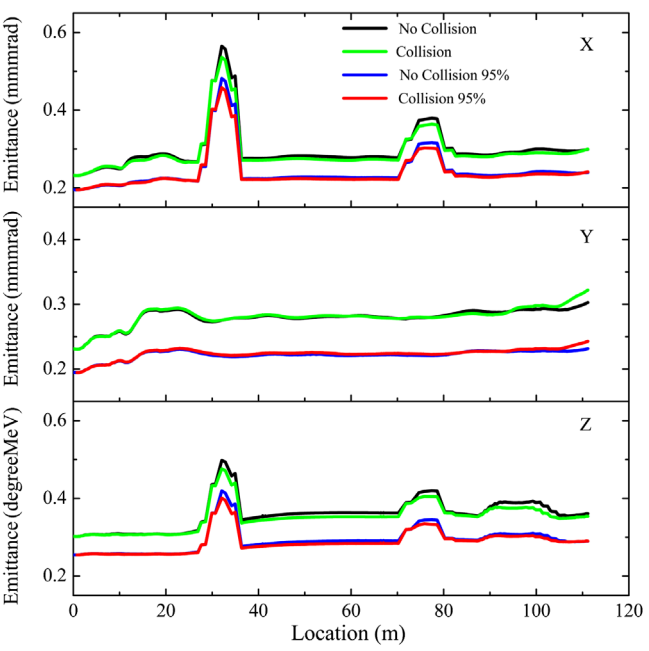

FIG. 7. The rms emittance and 95% percent emittance evolution of the single-bunch simulation and the simulation including multiple collisions through the double-pass linac.

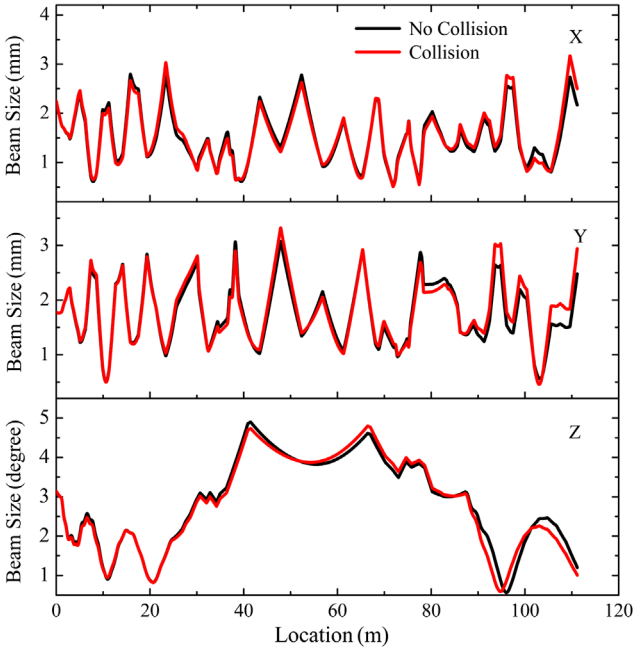

FIG. 8. The rms size evolution of the single-bunch simulation and the simulation including multiple collisions through the double-pass linac.

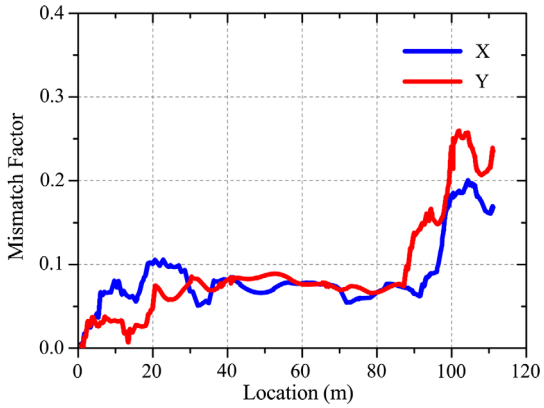

FIG. 9. Mismatch factor evolution of the single-bunch simulation and the simulation including multiple collisions through the double-pass linac.

code to the initial particle distribution of the IMPACT-T code. The low-energy bunch was then advanced forward a short distance so that the low-energy bunch phase adding multiple 2π's is the same as the phase of the high-energy bunch.

The longitudinal evolution of two bunch centroids during one two-bunch overtaking collision process is shown in Fig. 4. Here, the high-energy bunch is located behind the low-energy bunch at the beginning. Both bunches see effectively the same rf-driven phase. After a few nanoseconds, the high-energy bunch catches up and collides with the low-energy bunch and overtakes the low-energy bunch in the rest of region. Figures 5 and 6 show the proton beam rms sizes and emittance evolutions in one of the collision regions (cavity 4) from the combined two-bunch simulations and from the single-bunch simulation using the IMPACT-T code. It is seen that the differences of the rms beam sizes and emittances without the interbunch space-charge effects (single bunch) and with the interbunch space-charge effects during the overtaking collision (combined bunches) are small (a few percent). This is even smaller than the rough analytical estimate in the preceding section, which does not include the self-consistent dynamic evolution of particle distributions.

B. Multiple collisional effects through the entire linac

After the low-energy bunch and the high-energy bunch exit the fifth collision region at the end of the sixteenth cavity, the two particle distributions are converted back to the IMPACT-Z code distributions and transported through the rest of linac separately. The high-energy bunch will transport through the rest of superconducting cavities and moves to the next section, while the low-energy bunch will transport through the first arc, the straight transport line that includes bunching cavities, and the second returning arc, becoming the high-energy bunch during the second pass of the superconducting linac section. The new high-energy proton bunch will collide with a fresh low-energy bunch at five locations in the superconducting linac. After the five collisions, the low-energy bunch is transported through the recirculating beam line, becomes another new

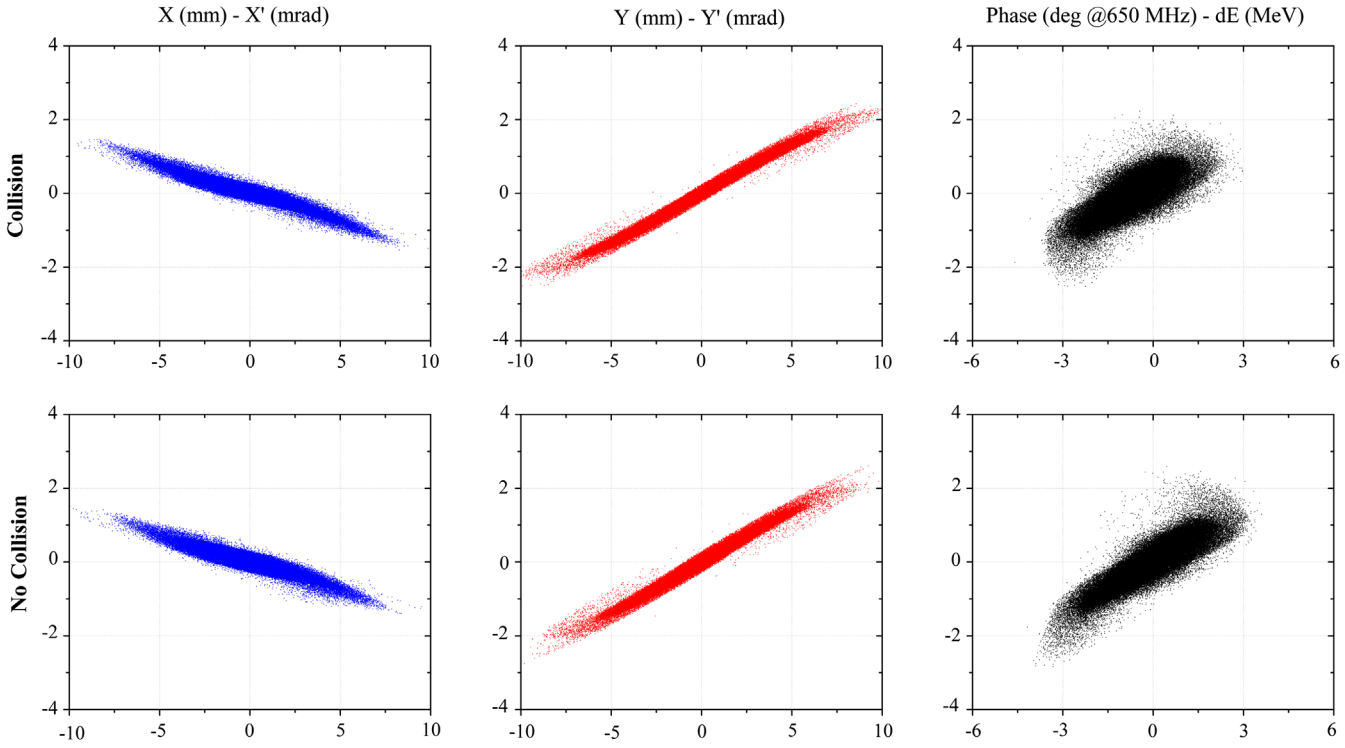

FIG. 10. Final transverse and longitudinal phase spaces at the end of the linac with and without the multiple collisions.

high-energy bunch, and goes through another five collisions with another fresh low-energy bunch. A single bunch will experience a total of ten collisions through the double-pass linac. The high-energy bunch used for the first five collisions already experienced five collisions during the first pass of the linac.

Figures 7–9 show the total rms emittance, 95% emittance, rms size, and mismatch factor evolution of a proton beam through the double-pass recirculating linac including multiple collisions. Here, the mismatch factor is defined as [10]

$$M = \sqrt{1 + \frac{\Delta + \sqrt{\Delta(\Delta+4)}}{2}} - 1, \tag{8}$$

where

$$\Delta = (\delta\alpha)^2 - \delta\beta\delta\gamma \tag{9}$$

and $\delta\alpha = \alpha - \alpha_0$, $\delta\beta = \beta - \beta_0$, and $\delta\gamma = \gamma - \gamma_0$ are the differences of the Twiss parameters with and without collisions. The evolution of those parameters with the original single bunch tracking (no collision) are also shown in the same figure. The relative differences of the rms beam size and the emittance between the bunch with overtaking collisions and the one without collisions are small during the first pass of the linac and grow somewhat during the second pass. The final relative differences at the end of the linac are still below 20% even after growth. The transverse mismatch factor of the proton through multiple collisions also increases during the second pass of the linac. However, the final mismatch factor at the end of the linac due to the collisions is still below 0.3. Figure 10 shows the final phase space distributions at the end of the linac with and without the ten collisions. Both the transverse and the longitudinal phase spaces look quite similar.

As a comparison, Tables III and IV also give the proton beam Twiss parameters at the end of the linac with and without collisional effects. It is seen that the proton beam Twiss parameters with ten overtaking collisions are still similar to those without being subject to a collision. The relative differences in all these Twiss parameters (rms beam size, momentum spread, alpha, and emittance) are less than 20%. This suggests that the interbunch space-charge effects during the overtaking collision would not dramatically change the beam property downstream.

TABLE III. Transverse Twiss parameters at the end of linac with and without collisions.

		Size (mm)	Momentum (mrad)	Alpha	Emittance (mm mrad)
X	Collision	2.50	0.38	3.53	0.30
	No collision	2.17	0.33	2.56	0.30
Y	Collision	2.94	0.80	−8.43	0.32
	No collision	2.48	0.70	−6.60	0.30

TABLE IV. Longitudinal Twiss parameters at the end of the linac with and without collisions.

		Size (deg)	Momentum (MeV)	Alpha	Emittance (deg MeV)
Z	Collision	1.01	0.58	1.24	0.35
	No collision	1.20	0.65	1.91	0.36

IV. CONCLUSIONS

The impact of space-charge effects during an overtaking collision on the proton beam quality in the cw double-pass recirculating superconducting proton linac was studied in this paper. Using an initial Gaussian distribution and 10 mA average current at rf 162.5 MHz frequency, we simulated a proton bunch transporting through the double-pass recirculating linac subject to five collisions during the first pass and five collisions during the second pass of the linac, including both the interbunch space-charge effects and the space-charge effects within the bunch itself, and compared the proton beam quality with that from a single-bunch beam dynamics tracking without a collision. The simulation results show no macroparticle losses during collisions and through the rest of linac with an aperture size of 8.3 cm in diameter [4]. The relative differences of the rms beam sizes and the emittance growth with and with collisions are small. This suggests that the overtaking collisions would not dramatically change the beam quality during the cw operation of the double-pass proton linac. In summary, this study shows that a 10 mA proton beam current under the cw operation of the double pass linac is feasible without extra hardware complexity. Such a facility can deliver a final 500 MeV cw proton beam and generate about 5 MW beam power. This MW-level proton driver would already be a valuable tool in applications such as a spallation neutron source and accelerator-driven nuclear energy production.

In future work, we will study the effects of machine imperfection on the proton beam quality in the double-pass recirculating superconducting linac and continue the beam dynamics design study of the second section of the proposed multi-GeV recirculating superconducting linac. The concept design of a phase shifter that can transport a proton beam four times while satisfying the phase synchronous condition for acceleration is also under way and will be reported in a future publication.

ACKNOWLEDGMENTS

This work was supported by the U.S. Department of Energy under Contract No. DE-AC02-05CH11231. One of the authors, Y. T., thanks China Scholarship Council for financial support (CSC File No. 201604910803). This research used some computer resources at the National Energy Research Scientific Computing Center.

[1] H. Abderrahim *et al.*, http://science.energy.gov/~media/hep/pdf/files/pdfs/ADS_White_Paper_final.pdf, 2010.
[2] Z. Li *et al.*, Physics design of an accelerator for an accelerator-driven subcritical system, Phys. Rev. ST Accel. Beams **16**, 080101 (2013).
[3] R. Pande, S. Roy, S. V. L. S. Rao, P. Singh, and S. Kailas, Physics design of a CW high-power proton Linac for accelerator-driven system, Pramana **78**, 247 (2012).
[4] S. Holmes *et al.*, Project X Document No. 776-v7, 2013.
[5] M. Eshraqi *et al.*, in *Proceedings of the 5th International Particle Accelerator Conference, IPAC2014, Dresden, Germany, 2014* (JACoW, Dresden, Germany, 2014), p. 3320.
[6] C. W. Leemann, D. R. Douglas, and G. A. Krafft, The continuous electron beam accelerator facility: CEBAF at the Jefferson Laboratory, Annu. Rev. Nucl. Part. Sci. **51**, 413 (2001).
[7] A. Richter, in *Proceedings of the Fifth European Particle Accelerator Conference, EPAC96, Sitges, Barcelona* (Institute of Physics Publishing, Bristol, Philadelphia, 1996), p. 110.
[8] J. Qiang, Wide energy bandwidth superconducting accelerating cavities, Nucl. Instrum. Methods Phys. Res., Sect. A **795**, 77 (2015).
[9] K. Hwang and J. Qiang, Beam dynamics simulation of a double pass proton linear accelerator, Phys. Rev. Accel. Beams **20**, 040401 (2017).
[10] Thomas P. Wangler, *RF Linear Accelerators*, 2nd ed. (Wiley, New York, 2008).
[11] J. Qiang, S. Lidia, R. D. Ryne, and C. Limborg, Three-dimensional quasistatic model for high brightness beam dynamics simulation, Phys. Rev. ST Accel. Beams **9**, 044204 (2006).
[12] J. Qiang, R. D. Ryne, S. Habib, and V. Decyk, An object-oriented parallel particle-in-cell code for beam dynamics simulation in linear accelerators, J. Comp. Physiol. **163**, 434 (2000).